Current Research (2015) Newfoundland and Labrador Department of Natural Resources Geological Survey, Report 15-1, pages 173-189

PRELIMINARY LITHOGEOCHEMISTRY FOR MAFIC VOLCANIC ROCKS FROM THE BONAVISTA PENINSULA, NORTHEASTERN NEWFOUNDLAND

A.J. Mills and H.A.I. Sandeman[1]
Regional Mapping Section
[1]Mineral Deposits Section

ABSTRACT

Lithogeochemical results are presented for 22 samples of mafic volcanic rocks from three distinct stratigraphic settings on the Bonavista Peninsula. Plagioclase porphyritic basalts from three prominent headlands in the Sweet Bay area are evolved, calk-alkaline basalts that have well-developed negative high-field-strength element (HFSE) anomalies and show the highest degree of lithospheric recycling. Mafic volcanic rocks of the Plate Cove volcanic belt are transitional to (weakly) calc-alkaline basalts, have variable Th/Nb and La/Nb relationships, and are derived from a lithosphere-contaminated, slightly enriched mid-ocean ridge basalt (E-MORB), shallow mantle source. Basalts exposed on the central-eastern part of the Bonavista Peninsula (Dam Pond basalt) have distinct ocean island basalt (OIB) chemistry, a minor lithospheric input as indicated by supra-asthenospheric Th/Nb values, and are clearly not correlative to the arc-like rocks of the Plate Cove volcanic belt, 30 km to the west.

INTRODUCTION

Rocks of the Bonavista Peninsula were initially attributed to the Neoproterozoic Musgravetown Group (Hayes, 1948; Rose, 1948; Christie, 1950; Jenness, 1963), until O'Brien and King (2002) demonstrated that significant parts, consisting of marine and deltaic siliciclastic rocks, were correlative with the Neoproterozoic units of the Avalon Peninsula: *i.e.*, the Conception–St. John's–Signal Hill groups (Figure 1). This last work resulted in the first documentation of the Ediacaran fossil assemblages at Catalina (O'Brien and King, 2002), initiation of biostratigraphic studies (O'Brien and King, 2004a; O'Brien *et al.*, 2006; Hofmann *et al.*, 2008), and provisional stratigraphic division of the Rocky Harbour and Crown Hill formations of the Musgravetown Group (O'Brien and King, 2004b, 2005). A new regional mapping initiative in 2009 (Normore, 2010) resulted in the modification of the proposed stratigraphy of O'Brien and King (2002, 2004b, 2005), and yielded preliminary geological maps of the Bonavista and Trinity areas (NTS map areas 2C/6 and 11; Normore, 2010, 2011). The current project builds upon the work of the earlier investigators to better understand the geology of the region and to ultimately produce 1:50 000-scale bedrock geology maps for the Bonavista and Trinity map areas.

O'Brien and King (2002) assigned much of the bedrock on the eastern side of the Bonavista Peninsula to the Conception Group. They later re-assigned rocks west of the Spillars Cove–English Harbour fault (SC–EH fault: Figure 2) to the Rocky Harbour Formation, Musgravetown Group (O'Brien and King, 2004b), and subsequently termed the Wilson Pond facies (O'Brien and King, 2005). Normore (2010), however, assigned these same siliceous rocks to the Big Head Formation of the Musgravetown Group (*see* McCartney, 1967 – Isthmus of Avalon area; *see* also King *et al.*, 1988 – Bay de Verde area; and Fletcher, 2006 – Cape St. Mary's area; Figure 1). The Big Head Formation was originally proposed for the grey-green, fine-grained sedimentary rocks that overlie the Bull Arm Formation (BAF) and are overlain by the redbeds of the Maturin Ponds Formation at Big Head, north of Long Harbour in Placentia Bay (McCartney, 1967). In the Long Harbour area and extending north of the isthmus along the west side of Trinity Bay, the Maturin Ponds Formation is overlain by olive green sandstone of the Trinny Cove Formation (correlative to the Hearts Content Formation in eastern Trinity Bay), which King *et al.* (1988) correlates with the Rocky Harbour Formation north of Random Sound (Figure 1; *see* stratigraphic column legend, King *et al.*, 1988). Normore (2010) interpreted these grey-green, fine-grained, siliceous, siliciclastic rocks to occupy a lower stratigraphic position than the Rocky Harbour Formation, although correlatives to the Maturin Ponds and Trinny Cove formations have not been identified on the Bonavista Peninsula. Designation to either the Wilson Pond facies (Rocky Harbour Formation of O'Brien and King, 2005), or the

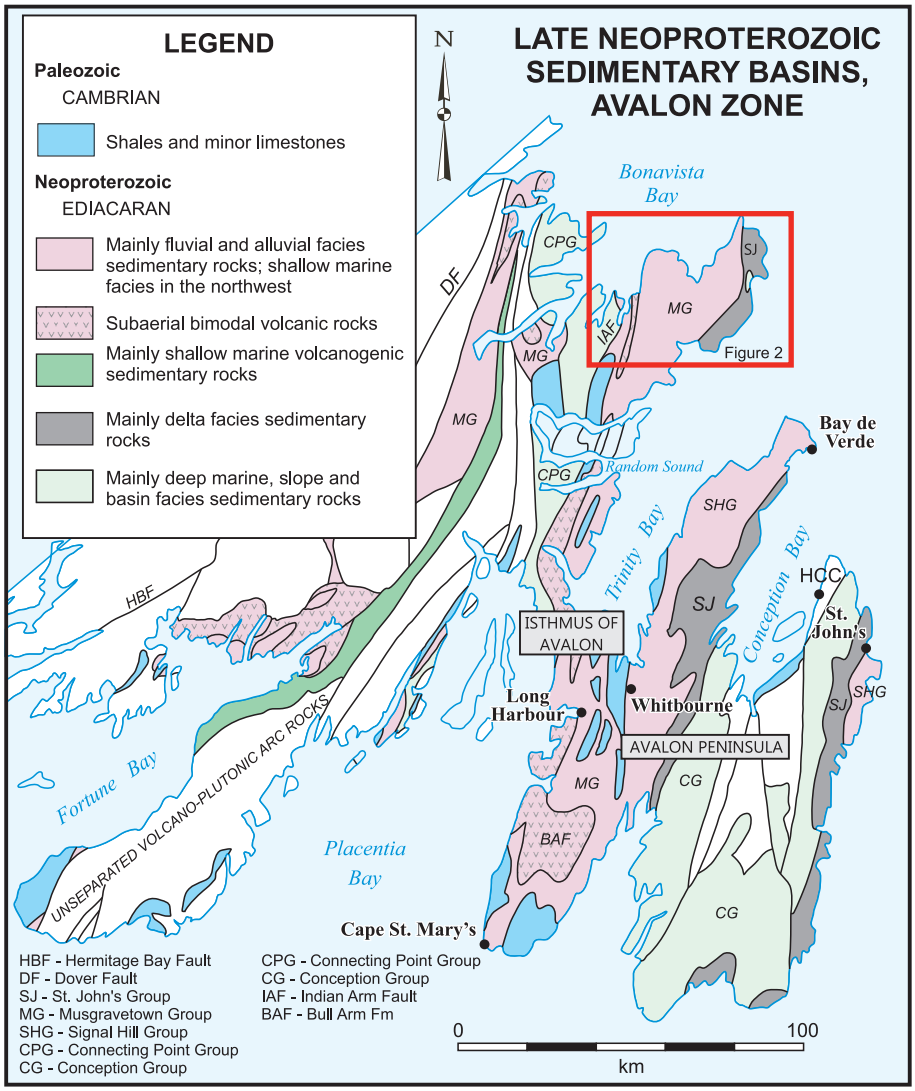

Figure 1. *Simplified geological map of the Avalon Zone of Newfoundland (modified from O'Brien and King, 2002) showing the distribution of maps units and location of Figure 2.*

stratigraphically lower Big Head Formation (Normore, 2010) presumes a stratigraphic position above the volcanic rocks of the Bull Arm Formation.

The BAF, first recognized by Hayes (1948), refers to the dominantly volcanic rock assemblage near the base of the Musgravetown Group (*see* Jenness, 1963; McCartney, 1967). Malpas (1972) investigated the volcanic rocks of the BAF at their type locality (near Isthmus of Avalon; Figure 1) and suggested, based on major element geochemistry and petrographic examination, an original calc-alkaline affinity, now chemically and mineralogically masked by metasomatism to produce keratophyre/spilite compositions.

The age of the BAF is poorly constrained. An age of 570 +5/-3 Ma reported from "rhyolite from the base of the Musgravetown Group" (O'Brien *et al.*, 1989) more accurately applies to "rhyolite flows at the base of the Rocky Harbour Formation" (O'Brien and King, 2004b), hence the age of the BAF must be older than *ca.* 570 Ma.

On the Bonavista Peninsula, three volcanic units are identified as possible correlatives to the BAF (Figure 2): 1) the Plate Cove volcanic belt (PCVB); 2) mafic volcanic rocks on the northern tips of three prominent headlands in the Sweet Bay area (Headland basalt: HB) and; 3) the Dam Pond basalt (DP). The PCVB has historically been correlated to the BAF (Hayes, 1948; Jenness, 1963; O'Brien, 1994; Mills, 2014) but this has not been petrogenetically corroborated. The HB has been previously interpreted as equivalent to the BAF (Hayes, 1948; Jenness, 1963; Mills, 2014), or, alternatively, as younger Siluro-Devonian volcanic rocks (O'Brien, 1994). The DP basalt has also been interpreted as equivalent to the BAF (Normore, 2010). This paper presents lithogeochemical data for mafic volcanic rocks of all three units, evaluates critical petrochemical differences and proposes plausible paleotectonic settings of formation.

FIELD AND PETROGRAPHIC DESCRIPTIONS

PLATE COVE VOLCANIC BELT (PCVB)

The PCVB, formerly considered to be BAF (Jenness, 1969; O'Brien, 1994; Mills, 2014), extends from the promontory at Plate Cove East, to approximately 20 km southward, beyond the limit of current field investigations (Figure 2). Basaltic rocks occur in the northern half of the belt where they are conformably overlain by red shale and felsic volcanic rocks (*e.g.*, Plate 1A; *see* also Mills, 2014) that include pyroclastic flows, tuffs and massive flow-banded rhyolitic domes that have brecciated aprons. The southern half of the belt is dominated by felsic pyroclastic rocks and flow-banded to massive rhyolite. The Indian Arm Fault separates the PCVB from the turbidite-dominated Connecting Point Group and possible Crown Hill Formation and overlying Cambrian units, to the west (Figure 2). Mafic vol-

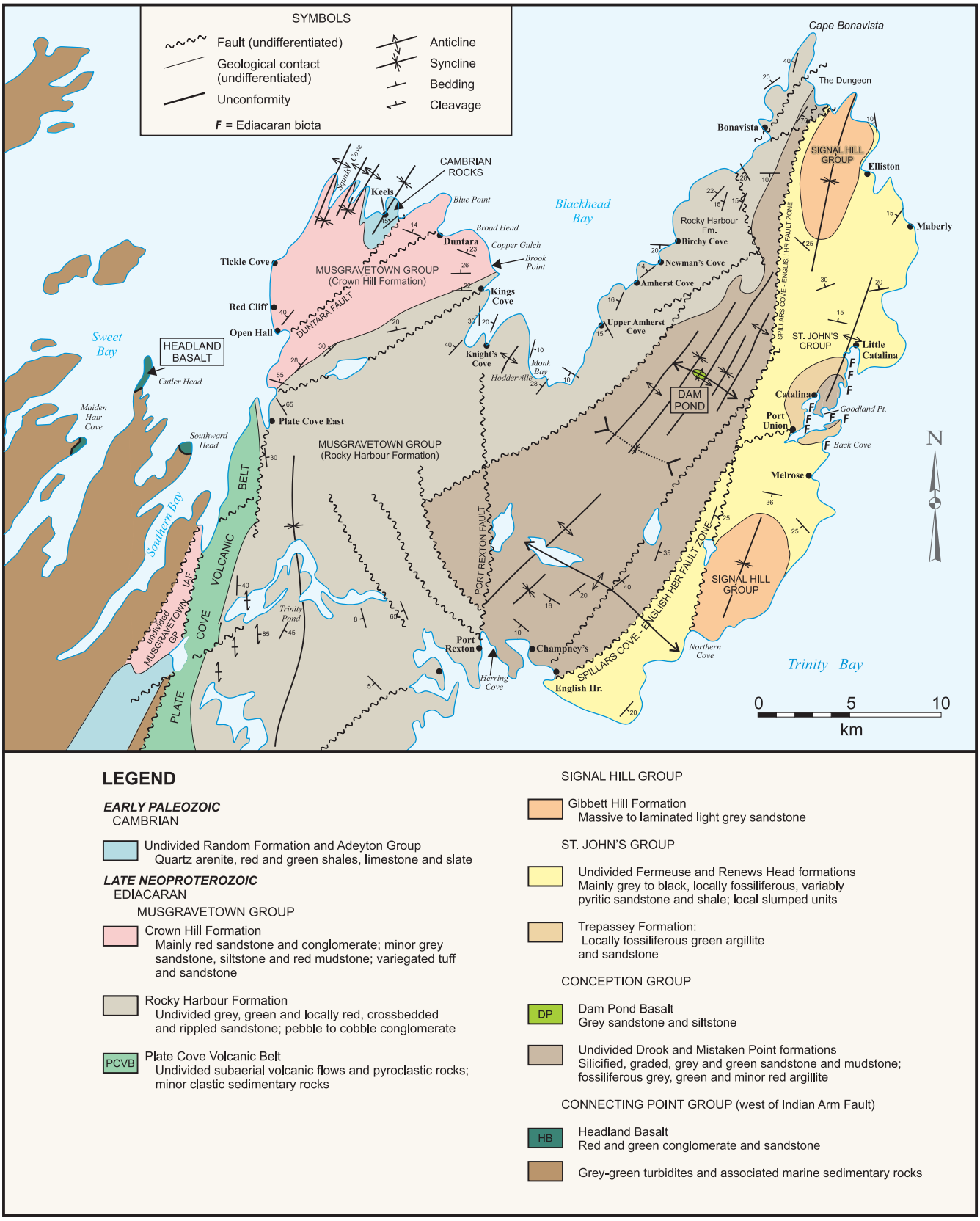

LEGEND

EARLY PALEOZOIC
CAMBRIAN

Undivided Random Formation and Adeyton Group
Quartz arenite, red and green shales, limestone and slate

LATE NEOPROTEROZOIC
EDIACARAN

MUSGRAVETOWN GROUP

Crown Hill Formation
Mainly red sandstone and conglomerate; minor grey sandstone, siltstone and red mudstone; variegated tuff and sandstone

Rocky Harbour Formation
Undivided grey, green and locally red, crossbedded and rippled sandstone; pebble to cobble conglomerate

PCVB — Plate Cove Volcanic Belt
Undivided subaerial volcanic flows and pyroclastic rocks; minor clastic sedimentary rocks

SIGNAL HILL GROUP

Gibbett Hill Formation
Massive to laminated light grey sandstone

ST. JOHN'S GROUP

Undivided Fermeuse and Renews Head formations
Mainly grey to black, locally fossiliferous, variably pyritic sandstone and shale; local slumped units

Trepassey Formation:
Locally fossiliferous green argillite and sandstone

CONCEPTION GROUP

DP — Dam Pond Basalt
Grey sandstone and siltstone

Undivided Drook and Mistaken Point formations
Silicified, graded, grey and green sandstone and mudstone; fossiliferous grey, green and minor red argillite

CONNECTING POINT GROUP (west of Indian Arm Fault)

HB — Headland Basalt
Red and green conglomerate and sandstone

Grey-green turbidites and associated marine sedimentary rocks

Figure 2. *Simplified map of the northern Bonavista Peninsula showing the regional distribution of rock units (modified from O'Brien and King, 2005). IAF = Indian Arm Fault*

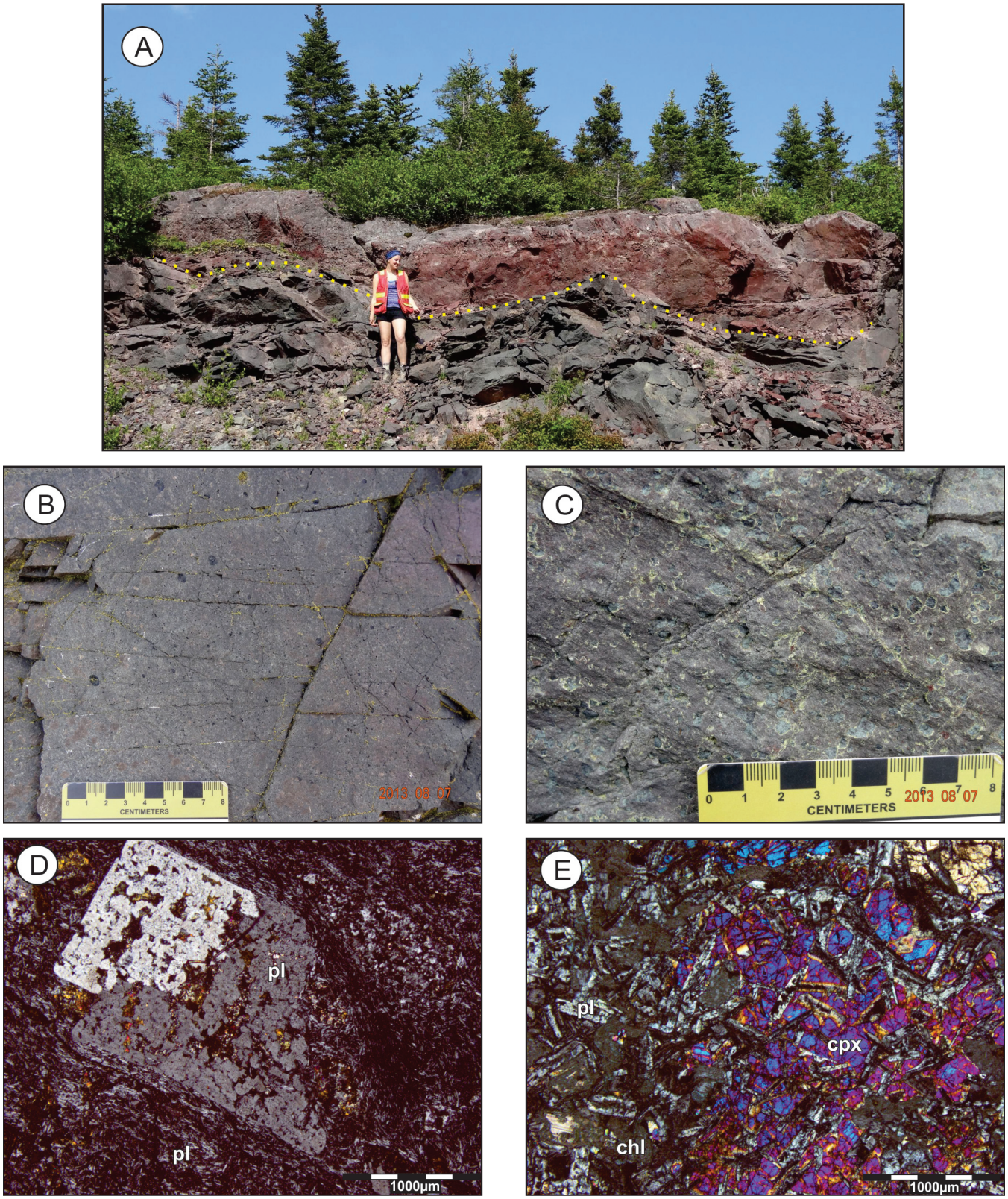

Plate 1. *Mafic rocks of the PCVB. A) Mafic volcanic rocks overlain by red mudstone and felsic volcanic rocks (view to the east; site of 13AM147A and B); person for scale is approximately 1.8 m in height; B) Chlorite amygdales in Plate Cove basalt (site of 13AM321C); C) Patchy epidote alteration in Plate Cove basalt, particularly at amygdale rims (site of 13AM325A);* D) *Sieve-textured plagioclase phenocryst enveloped by trachytic/flow texture (sample 13AM321C); and E) Subophitic texture: randomly oriented plagioclase laths in optically continuous* (i.e., *probably single crystal) clinopyroxene (sample 13AM001A). pl = plagioclase; cpx = clinopyroxene; chl = chlorite.*

canic rocks range from grey to maroon and are generally aphyric at the base of individual flows and amygdaloidal toward the top. Well-developed flow-top breccia is locally preserved. Amygdales are dominated by chlorite or carbonate, with abundant epidote locally (Plate 1B, C).

Lithogeochemical investigations reveal two chemically distinct groups of basaltic rocks within the PCVB, herein differentiated as subunits $PCVB_1$ and $PCVB_2$ (*see* 'Classification and lithochemistry' section). Both series and individual samples exhibit variable chlorite, epidote, sericite and carbonate alteration. Fine-grained epidote is locally present in the matrix of some samples, whereas others have patchy chlorite alteration or, more rarely, carbonate and sericite alteration of matrices. Amygdales in one of the $PCVB_1$ samples (10LN013A) contains quartz and epidote and is rimmed by radiating adularia crystals. Chlorite-filled amygdales are commonly about 5 mm in diameter, and quartz–epidote amygdales are locally abundant but typically smaller. Subhedral, sieve-textured plagioclase phenocrysts (≤4 mm long), enveloped by a variably trachytic-textured, fine-grained, plagioclase-rich matrix (Plate 1D) occur in both series but are more common in subunit $PCVB_1$. Two samples of subunit $PCVB_2$ (13AM001A and 13AM147A) contain clinopyroxene crystals, 3–4 mm in diameter, that range from nearly pristine euhedral prisms to fractured and fragmented anhedral grains with variable chlorite alteration. In these samples, plagioclase chadacrysts occur in clinopyroxene grains that are up to 1 mm long, forming subophitic and ophitic textures (Plate 1E). Trace magnetite locally exhibits exsolution lamellae of ilmenite (not probe-confirmed), and is locally altered to hematite. Anhedral chalcopyrite, 10 to 50 μm in diameter, is also locally present.

SWEET BAY HEADLAND BASALT (HB)

The northern tips of three prominent headlands in the Sweet Bay area (Figure 2) are underlain by mafic volcanic flows intercalated with minor red and green sandstone, red shale and red and green pebble conglomerate at m- to da-scale. At Southward Head, the easternmost of the three headlands, the basalt flows conformably overlie red conglomerate and minor felsic tuff and these collectively overlie, with angular unconformity, the green-grey to variegated rocks of the uppermost Connecting Point Group (Kate Harbour formation of Mills, 2014: *see* Plate 12, Mills, 2014). On the west side of Southward Head, the basal red conglomerate and interbedded tuff are not preserved (possibly because they have been removed by later faulting), and steeply dipping rocks of the upper Connecting Point Group are directly overlain by a shallowly north-dipping basalt flow (Plate 2A). The HB succession also occurs at Cutler Head and Maiden Hair Cove and, in both cases, is fault-bounded against rocks of the Connecting Point Group (Mills, 2014).

The HB is locally amygdaloidal (Plate 2B) and commonly plagioclase glomerocrystic (Plate 2C). The glomerocrysts comprise approximately 30% of the rock and average 5 mm in diameter. Plagioclase is typically highly saussuritized, however, remnant oscillatory zoning is locally preserved (Plate 2D). Mafic minerals are minor, although magnetite locally comprises up to 3 modal % (Plate 2E). The matrix, now composed predominantly of chlorite, may have been originally glassy. These rocks differ from basalts of the PCVB in that they lack clinopyroxene and chlorite and contain plagioclase glomerocrysts and up to 3% magnetite.

DAM POND BASALT (DP)

Mafic volcanic rocks are exposed along the shoreline of a small pond (named Dam Pond by previous workers) located on the south side of Highway 237, approximately midway between Catalina and Upper Amherst Cove (Figure 2; Plate 3A). Normore (2010) defined the aerial extent of these rocks and proposed that they are correlative with the PCVB located 30 km to the west. He assigned the overlying green-grey siliceous rocks to the Big Head Formation of McCartney (1967; Whitbourne area; Figure 1).

The basalts at Dam Pond are poorly exposed, dark- to light-green, vesicular to amygdaloidal massive flows. Fragmental mafic volcanic rocks crop out on a small island near the south side of Dam Pond and flow banding is evident in some of the larger fragments (Plate 3B). The basalts contain relict, subhedral clinopyroxene up to 2 mm long, which is commonly resorbed and variably altered to chlorite (Plate 3C and D). Plagioclase exhibits a bimodal size distribution, with <1 mm phenocrysts and 100 to 200 μm laths in the groundmass. Amygdales average 2 mm in diameter and are filled with chlorite±carbonate±quartz±epidote. In thin section, clasts of fine-grained basalt that have very fine-grained, chilled rims and contain calcite and/or chlorite amygdales were noted, demonstrating the petrogenetic complexity of some of these rocks. Two samples (09LN314A and 09LN554A) have adularia ± quartz ± epidote amygdales (Plate 3E). The matrix of most samples contains patches of chlorite-alteration and 30–50 μm titanite grains are commonly spatially associated with the alteration (Plate 3F). It is unclear if the chlorite alteration is deuteric (*i.e.*, due to late-exsolved fluids related to eruption) or metamorphic in origin.

ANALYTICAL METHODS

The lithogeochemical study aims to characterize the compositional variations of mafic volcanic rocks and to provide insight into their origin. Representative samples that are devoid of weathering, and free of veins and fractures were collected. Samples were analyzed for their major- and select trace-element contents by Inductively Coupled Plas-

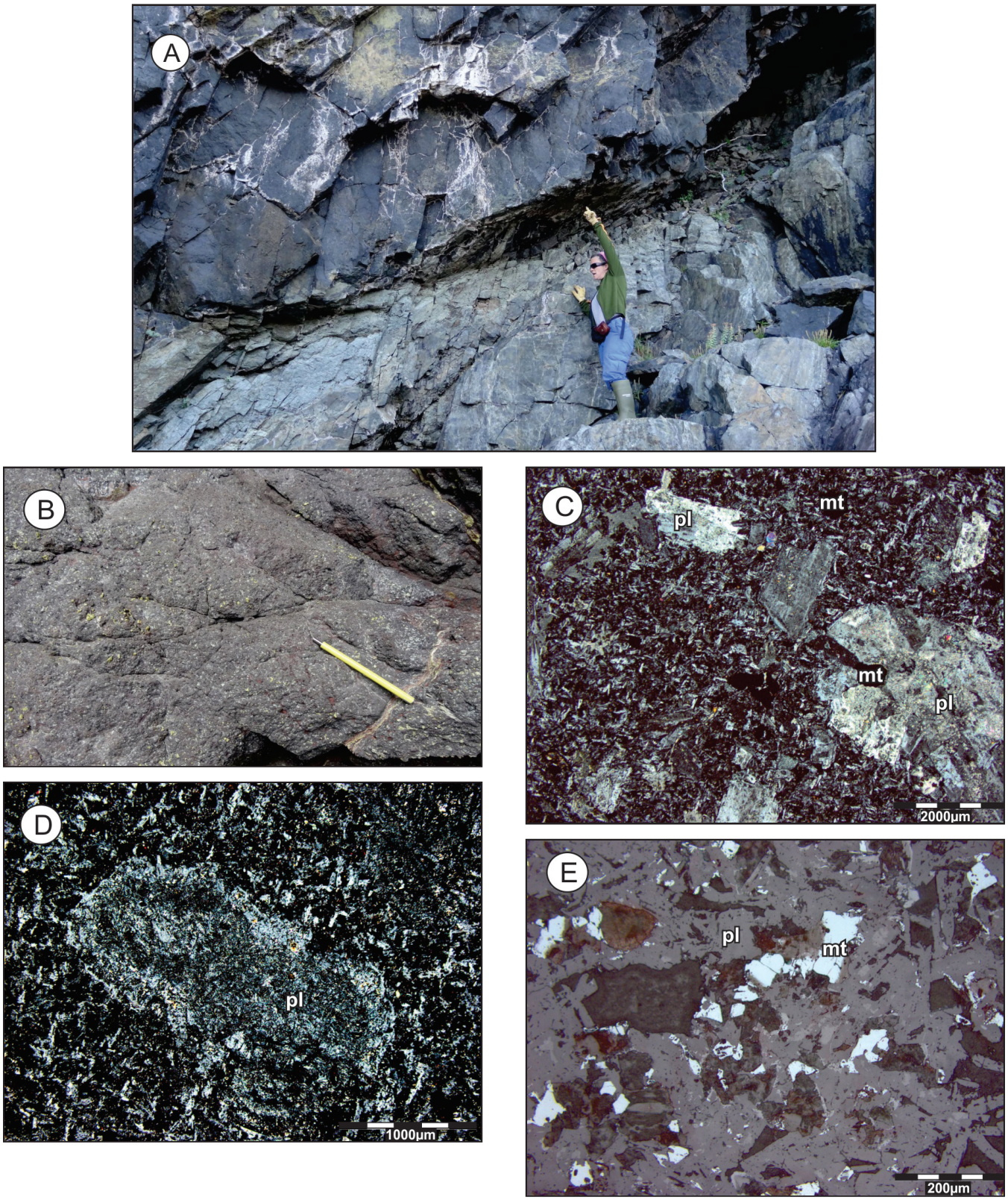

Plate 2. *Mafic rocks of the Sweet Bay headlands. A) Mafic volcanic rock overlying steeply dipping, grey sandstone of the Connecting Point Group, west side of Southward Head (13AM313A; view to the north); person for scale is approximately 1.5 m in height; B) Plagioclase glomerocrystic and carbonate amygdaloidal basalt from west side of Southern Bay Head (13AM312A); C) Saussurite-altered plagioclase glomerocrystic basalt in cross-polarized light (13AM312A); D) Relict zoning (brighter rim relative to core) in plagioclase phenocryst (cross-polarized light; west side of Cutler Head; 13AM335A); and E) Common magnetite in the matrix of most Headland basalts (reflected light; 13AM312A). pl = plagioclase; mt = magnetite.*

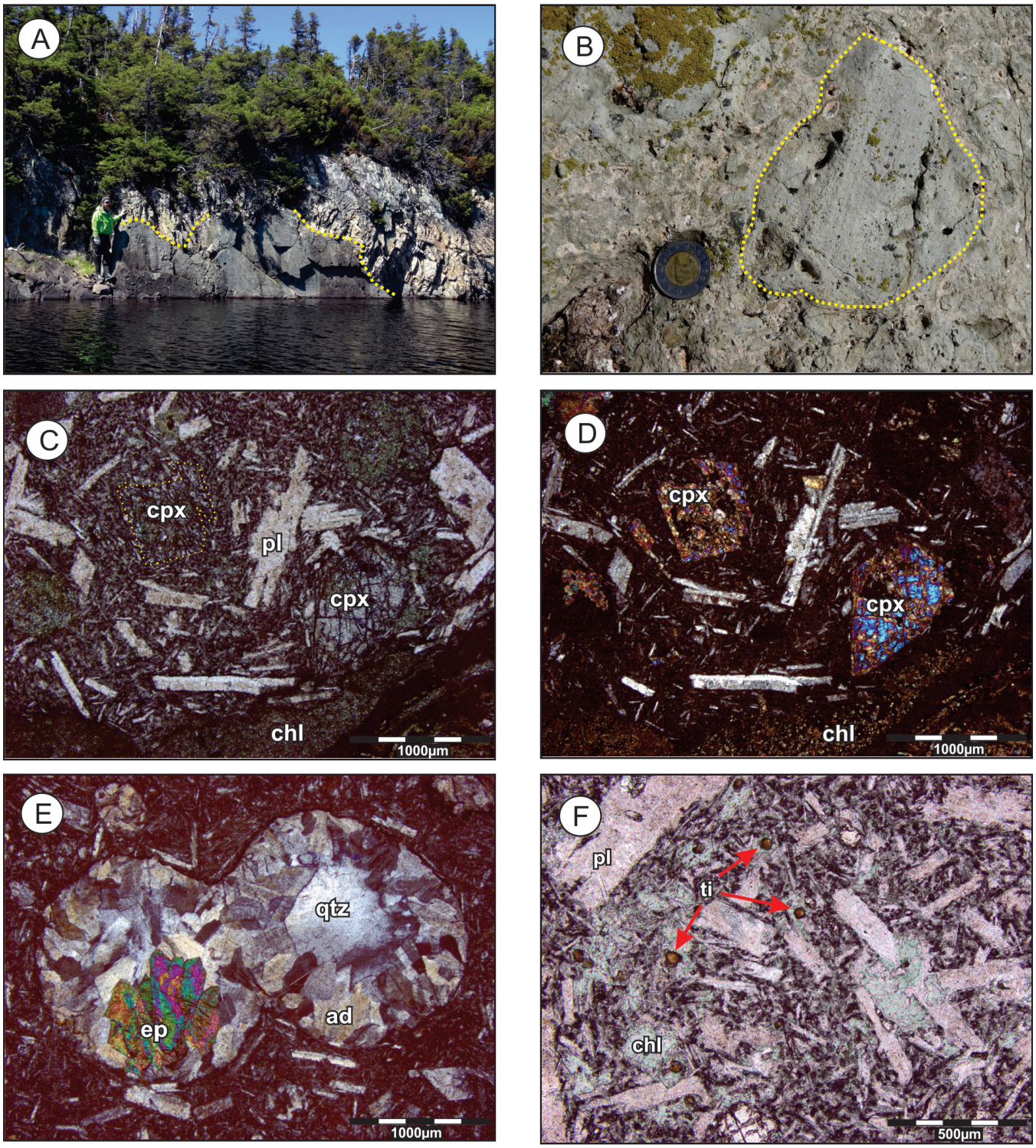

Plate 3. *Mafic volcanic rocks of the Dam Pond area. A) Irregular surface of Dam Pond mafic volcanic rock overlain by white-weathering, fine-grained, grey sandstone and siltstone that dips gently to the northeast (view to the north; 14AM041A); person for scale is approximately 1.8 m in height; B) Cobble-size mafic volcanic fragment showing flow texture, on a small island near the southern shore of Dam Pond (14AM039); C) Partially resorbed, subhedral, relict clinopyroxene in Dam Pond basalt, plane-polarized light (09LN314A); D) Partially resorbed, subhedral, relict clinopyroxene in Dam Pond basalt, cross-polarized light (09LN314A); E) Adularia, quartz and epidote in fused amygdales (sample 09LN314A); and F) Titanite grains associated with chlorite alteration in Dam Pond basalt (14AM041A). cpx = clinopyroxene; pl = plagioclase; chl = chlorite; qtz = quartz; ep = epidote; ad = adularia; ti = titanite.*

ma Optical Emission (ICP-OES) and Mass Spectrometry (ICP-MS) at the Geochemical Laboratory, Department of Natural Resources, Government of Newfoundland and Labrador. Pulverized sample material was fused at 1000^{O}C in a graphite crucible for 30 minutes using a flux mixture of Lithium Borates. The molten fusion bead was poured directly into a 10% solution of nitric acid, stirred for approximately 15 minutes until dissolution, then made to a final volume of 100 ml (C. Finch, personal communication, 2014). An aliquot of this solution was measured directly by a Thermo Instruments iCap 6500 Inductively Coupled Plasma Optical Emission Spectrometer (ICP-OES) for major- and trace-element abundances (Table 1). Analytical methods outlined in Finch (1998) apply for FeO and LOI determinations. A set of 23 samples of mafic volcanic rocks were analyzed (Table 1).

CLASSIFICATION AND LITHOGEOCHEMISTRY

MAJOR- AND TRACE-ELEMENT GEOCHEMISTRY

All three mafic volcanic units described earlier display overlapping compositional ranges from tephrite/basanite through basalt and trachy-basalt to basaltic trachy-andesite on the total alkalis *vs* silica diagram from Le Bas *et al.* (1986; Figure 3). Rocks of the PCVB show a greater compositional range than the DP or HB (possibly an artifact from the small number of samples analyzed). The variability in major element chemistry of the PCVB is likely a result of secondary or deuteric alteration of the rocks, as observed in thin section. Many of the samples are visibly altered, indicating that their compositions may have been modified by late- or post-crystallization fluid-rock interactions. Such alteration may result in modification and mobilization of the more mobile major and trace elements, however, it typically has little effect on the immobile trace elements (Pearce and Cann, 1973; Wood, 1980; Middelburg *et al.*, 1988). This is illustrated in Figure 4, which highlights that many of the samples have been affected by the addition or loss of Na. This is also indicated by the relatively high LOI from most altered samples and the relatively high (>5) Al_2O_3/Na_2O index (Spitz and Darling, 1978) in one sample of each rock unit (Table 1). Care must be taken when interpreting the major- and mobile-element chemistry because many of the samples have been affected by alteration. For these reasons, we base the lithogeochemical interpretation of the rocks on the relatively immobile trace elements, including the high-field strength elements (HFSE) and the rare-earth elements (REE).

To classify the mafic volcanic rocks we use the incompatible trace-element classification scheme for altered volcanic rocks (Figure 5: Pearce, 1996), which indicates that samples from both the PCVB and HB are subalkaline basalts, whereas samples from Dam Pond are alkali basalts. It is also apparent that the Plate Cove rocks form two distinct series on the basis of their Nb/Y ratios: subunit $PCVB_1$ has higher Nb/Y than subunit $PCVB_2$.

On element-element plots, samples of $PCVB_1$ and $PCVB_2$ basalts show weak trends of decreasing MgO with increasing Zr and fractionation (Figure 6A), typical of basaltic rocks. Subunit $PCVB_1$ shows a negative correlation between TiO_2 and Zr whereas $PCVB_2$ exhibits a positive correlation (Figure 6B). Well-defined positive linear correlations are evident for most highly immobile elements, as illustrated by the Th *vs* Zr (Figure 6C) and the Y *vs* Zr plots (Figure 6D).

In contrast, Zr concentrations exhibit little variation in both the Dam Pond and Headland basalts, making fractionation trends less clear, particularly with respect to the major elements. A weak positive correlation is apparent between TiO_2 and Zr in both the Dam Pond and Headland basalts (Figure 6B). Both display positive correlations for most highly incompatible elements, as shown in Figures 6C and D.

All three mafic volcanic sets from the Bonavista Peninsula exhibit moderate-to-low Mg#'s (19.0–62.9) as well as Cr (3–217 ppm) and Ni (10–100 ppm) concentrations (Figure 7), significantly lower than primary, mantle-derived melt compositions (Roeder and Emslie, 1970; Ringwood, 1975).

All three mafic volcanic units plot as distinct groups on incompatible trace element discrimination diagrams (*e.g.*, Cabanis and Lecolle, 1989; Wood, 1980: Figure 8A, B). The Dam Pond basalts plot in the ocean island basalt (OIB) field of Wood (1980), and within the 'continental' field of the ternary diagram of Cabanis and Lecolle (1989), and have relatively elevated Nb, consistent with eruption in an intraplate setting. Basalts from the Sweet Bay headlands are evolved arc-basalts (Figure 8A; Wood, 1980) and calc-alkaline basalts (Cabanis and Lecolle, 1989; Figure 8B), consistent with an orogenic tectonic setting. Less clear, in terms of tectonomagmatic origin, are the rocks of the PCVB. Both series plot along an array between arc-basalt and normal mid-ocean ridge basalt/enriched mid-ocean ridge basalt (N-MORB/E-MORB) (Figure 8A; Wood, 1980) and, therefore, appear to be transitional, arc-like to MORB-like basalts. Similarly, the PCVB rocks straddle the boundary between calc-alkaline and continental rocks in the diagram of Cabanis and Lecolle (1989), but have much higher relative Y abundances than the other volcanic units (Figure 8B).

Note: Table revised: *see* Mills and Sandeman, Current Research, 2019.

Table 1. Lithogeochemical data for mafic volcanic rocks from the Bonavista Peninsula. All oxides are in weight % whereas trace elements are given in ppm. UTM coordinates are in NAD27, Zone 22 format. Key: HB = Headland basalts; $PCVB_1$ = Plate Cove series 1; $PCVB_2$ = Plate Cove series 2; DP = Dam Pond basalt. FeO^T – total iron as ferrous iron; < = concentration is below the given detection limit; N/A = not analyzed; CIA = chemical index of alteration = $[Al_2O_3/(Al_2O_3+CaO+Na_2O+K_2O)]*100$ (Nesbitt and Young, 1982); Mg# = $MgO/MgO+FeO^T)*100$; CN subscript denotes chondrite normalized ratios; 13AM301A* is a duplicate analysis of 13AM301A. Please note that some elements have differing detection limits depending on interference from other elements

Sample	D.L.	13AM301A	13AM301A*	13AM312A	13AM335A	13AM410A	13AM001B	13AM321C	13AM386A	10LN013A	13AM001A	13AM147A
EASTING		304816	304816	310809	308025	310607	311408	312952	313232	313025	311408	311046
NORTHING		5374238	5374238	5373755	5377466	5373622	5367848	5373095	5370614	5370153	5367848	5363023
MAPUNIT		HB	HB	HB	HB	HB	$PCVB_1$	$PCVB_1$	$PCVB_1$	$PCVB_1$	$PCVB_2$	$PCVB_2$
Lithology		basalt flow	basalt flow	basalt flow	basalt flow	basalt flow	basalt flow	basalt flow	basalt flow	basalt flow	basalt dyke	basalt flow
SiO_2	0.01	46.51	46.88	50.10	46.71	47.43	55.93	55.87	48.63	46.19	46.95	45.41
TiO_2	0.001	1.02	1.40	1.20	1.01	1.19	1.75	1.57	1.92	1.96	1.87	1.45
Al_2O_3	0.01	16.68	17.87	18.16	19.39	18.66	15.17	16.40	15.64	15.55	14.88	16.55
FeO^T		10.27	11.66	10.54	8.83	10.12	8.89	8.43	10.09	11.41	11.17	10.58
$Fe_2O_3^T$	0.01	11.41	12.96	11.72	9.82	11.25	9.88	9.37	11.22	12.68	12.41	11.76
Fe_2O_3	0.01	9.05	8.74	9.67	8.07	8.82	6.08	7.88	6.57	9.04	2.20	5.35
FeO	0.01	2.12	3.80	1.84	1.57	2.19	3.42	1.34	4.18	3.27	9.19	5.77
MnO	0.001	0.17	0.22	0.19	0.17	0.18	0.13	0.28	0.22	0.26	0.21	0.28
MgO	0.01	1.35	6.45	4.46	3.10	3.22	3.27	2.14	6.98	7.55	9.53	8.39
CaO	0.01	17.37	2.40	2.77	5.61	6.46	4.57	2.38	4.57	3.52	5.85	5.21
Na_2O	0.01	0.21	4.48	5.45	4.04	4.25	6.90	6.76	5.18	3.02	4.05	3.15
K_2O	0.01	0.30	2.07	1.86	2.91	1.60	0.68	1.48	0.71	3.96	0.21	2.12
P_2O_5	0.001	0.43	0.53	0.42	0.48	0.44	0.34	0.59	0.39	0.30	0.28	0.41
Cr	1	11	16	23	8	22	80	3	91	103	217	123
Zr	1	97	128	111	121	108	254	327	260	183	124	106
Ba	1	117	1326	1082	1523	946	140	1359	467	867	114	766
LOI	0.01	2.73	3.73	3.20	4.88	3.38	1.09	1.37	2.94	4.28	3.98	4.28
Total		98.18	98.99	99.52	98.12	98.05	99.72	98.22	98.41	99.26	100.22	99.02
CIA		48.26	66.62	64.30	60.70	60.27	55.53	60.71	59.91	59.70	59.55	61.25
Mg#		18.98	49.66	42.98	38.51	36.15	39.56	31.18	55.23	54.12	60.32	58.57
Al_2O_3/Na_2O		78.80	3.99	3.33	4.80	4.40	2.20	2.43	3.02	5.16	3.68	5.25
V	5	273	349	317	305	373	205	34	244	226	251	292
Co	1	28	33	32	26	28	36	8	42	55	56	44
Ga	1	22	14	17	24	19	15	24	20	21	15	17
Ge	1	6	3	3	4	3	4	4	3	4	3	4
As	5	15	<5	<5	<5	<5	<5	6	<5	6	<5	<5
Sr	1	4003	591	649	551	506	142	207	188	163	57	411
Y	1	17.1	22.3	19.1	18.9	20.4	34.6	49.6	40.4	26.2	24.4	24.4
Nb	1	6.2	7.4	6.6	8.4	9.4	14.5	18.4	14.3	13.9	5.8	6.4
Mo	2	<2	<2	<2	<2	<2	<2	1.7	1.7	97.3	<2	2.4
Cd	0.2	<0.2	<0.2	<0.2	<0.2	0.2	<0.2	<0.2	<0.2	<0.1	<0.2	<0.2
Li	1	N/A	N/A	N/A	N/A	N/A	N/A	N/A	N/A	68.7	N/A	N/A
In	0.2	<0.2	<0.2	<0.2	<0.2	<0.2	<0.2	<0.2	<0.2	N/A	<0.2	<0.2
Sn	1	1.7	0.6	1.7	2.8	2.7	1.3	3.6	3.2	1.8	<1	0.7
Cs	0.5	<0.5	0.9	0.5	1.0	0.7	<0.5	<0.5	0.6	2.1	<0.5	0.6
Be	0.1	0.8	0.4	1.1	2.0	1.6	3.7	5.0	1.5	0.5	0.5	1.0
Cu	1	11555	25	124	705	55	56	3	55	<1	68	20
Li	0.1	20	58	43	22	34	15	18	48	<1	28	66
Mn	1	1151	1471	1270	1171	1258	884	1964	1490	1939	1401	1957
Ni	1	24	26	25	19	24	44	10	49	54	100	68
Pb	<1	<1	<1	<1	<1	2	<1	<1	<1	<1	<1	<1
Rb	1	9	91	88	153	81	23	38	25	110	6	29
Sc	0.1	26	38	30	21	29	30	29	31	39	37	33
Ti	1	6291	8682	7462	6402	7413	10904	9625	11915	12420	10759	9025
Zn	1	61	102	99	79	84	60	192	115	113	98	94
La	0.5	25.30	33.35	30.20	36.19	32.51	21.67	24.47	25.41	13.06	10.38	14.84
Ce	0.5	53.78	75.56	65.94	74.85	66.30	48.24	63.69	57.52	37.34	25.20	34.58
Pr	0.1	6.99	9.62	8.53	9.35	8.44	6.36	8.41	7.80	4.34	3.74	4.68
Nd	0.2	30.76	41.76	36.53	40.33	37.00	29.05	39.46	33.73	20.14	17.93	21.63
Sm	0.1	6.01	8.62	7.63	8.13	6.92	6.85	10.55	7.81	4.93	4.76	5.43
Eu	0.1	1.59	2.24	1.81	2.05	2.11	1.72	4.22	2.16	1.53	1.32	1.67
Tb	0.1	0.67	0.89	0.82	0.83	0.75	1.02	1.71	1.31	0.89	0.76	0.83
Gd	0.1	4.96	6.85	5.75	6.15	6.19	6.57	10.53	7.98	5.97	4.95	5.08
Dy	0.1	3.56	4.68	4.36	4.08	3.94	6.81	10.08	7.69	5.17	5.03	4.81
Ho	0.1	0.65	0.83	0.74	0.72	0.73	1.29	1.97	1.48	1.12	0.89	0.95
Er	0.1	1.83	2.35	2.12	2.03	2.25	3.73	5.62	4.41	3.24	2.81	2.71
Tm	0.1	0.24	0.32	0.28	0.25	0.29	0.54	0.73	0.62	0.45	0.33	0.37
Yb	0.1	1.66	2.19	1.96	1.74	1.78	3.67	5.01	4.06	3.03	2.41	2.24
Lu	0.1	0.23	0.31	0.27	0.26	0.31	0.54	0.81	0.63	0.43	0.34	0.35
Hf	0.2	2.65	3.68	3.26	3.33	3.12	6.24	8.58	7.09	4.49	3.16	2.78
Ta	0.5	0.61	0.60	<0.5	0.56	<0.5	0.99	2.29	1.07	0.61	<0.5	0.63
W	1	2.54	1.39	2.01	1.23	1.49	<1	2.66	1.10	1.44	2.29	1.78
Tl	0.1	<0.1	<0.1	<0.1	<0.1	<0.1	<0.1	<0.1	<0.1	0.39	<0.1	<0.1
Bi	0.4	<0.4	<0.4	<0.4	<0.4	0.55	0.62	<0.4	<0.4	N/A	<0.4	<0.4
Th	0.1	7.89	10.84	8.81	11.77	8.92	3.30	5.49	3.80	2.09	0.89	0.70
U	0.1	1.59	2.11	1.66	2.64	1.94	1.06	1.84	1.25	0.79	0.34	0.26

Table 1. Continued

Sample	13AM147B	13AM194A	13AM325A	13AM390C	09LN313A	09LN314A	09LN554A	09LN555A	09LN560A	14AM041A	10LN002A	10LN003A
EASTING	311046	314371	311627	312026	340928	340878	340579	340590	340492	340974	340897	340819
NORTHING	5363023	5376285	5368265	5369278	5377329	5377301	5377431	5377365	5376806	5377286	5377311	5377301
MAPUNIT	$PCVB_2$	$PCVB_2$	$PCVB_2$	$PCVB_2$	DP	DP	DP	DP	DP	DP	DP	DP
Lithology	basalt flow	basalt flow	basalt flow	basalt flow	basalt flow	basalt flow	basalt flow	basalt flow	basalt flow	basalt flow	basalt flow	basalt flow
SiO_2	46.17	43.27	45.42	52.17	47.46	50.90	44.06	43.99	53.32	47.55	47.56	46.10
TiO_2	1.52	2.82	1.95	2.59	1.78	1.51	1.67	1.71	1.72	1.63	1.74	1.80
Al_2O_3	16.34	13.92	17.30	13.68	17.57	15.92	15.82	16.08	17.13	15.03	16.54	16.38
FeO^T	10.16	13.18	11.42	10.29	9.53	6.29	9.05	8.78	9.70	8.94	9.19	8.97
$Fe_2O_3^T$	11.29	14.65	12.69	11.44	10.59	7.00	10.06	9.76	10.78	9.93	10.22	9.97
Fe_2O_3	4.46	7.83	6.12	6.75	2.99	1.65	1.60	1.37	2.52	2.03	2.82	2.12
FeO	6.15	6.14	5.91	4.22	6.84	4.81	7.62	7.55	7.43	7.11	6.66	7.07
MnO	0.29	0.37	0.23	0.27	0.41	0.19	0.35	0.31	0.27	0.23	0.24	0.27
MgO	8.78	8.76	8.04	4.37	6.24	5.56	5.99	6.85	4.44	8.49	7.10	7.38
CaO	4.67	5.13	6.04	4.62	3.70	5.39	6.20	7.41	2.66	6.48	4.89	6.37
Na_2O	3.47	4.11	3.66	5.27	5.24	3.50	2.39	4.81	5.43	4.38	4.29	4.83
K_2O	1.74	0.12	0.45	0.45	1.37	4.28	4.19	0.76	0.61	0.54	1.44	0.62
P_2O_5	0.43	0.40	0.41	0.78	0.65	0.58	0.52	0.61	0.56	0.55	0.55	0.68
Cr	127	154	156	16	185	157	177	198	37	174	189	205
Zr	112	181	140	221	207	160	181	179	214	176	183	193
Ba	564	35	462	372	310	1889	1722	195	154	153	602	192
LOI	4.34	5.24	4.38	2.94	5.10	4.13	7.11	8.00	3.78	5.06	4.48	6.22
Total	99.05	98.79	100.56	98.58	100.14	98.95	98.37	100.29	100.71	99.87	99.05	100.61
CIA	62.31	59.80	63.00	56.95	63.00	54.74	55.30	55.33	66.32	56.87	60.87	58.09
Mg#	60.63	54.23	55.66	43.08	53.85	61.13	54.10	58.15	44.92	62.87	57.92	59.45
Al_2O_3/Na_2O	4.70	3.39	4.72	2.60	3.35	4.55	6.61	3.34	3.16	3.43	3.85	3.39
V	278	430	293	261	205	170	195	262	170	199	225	198
Co	45	56	52	23	42	35	42	34	35	35	43	48
Ga	17	26	17	26	25	15	19	22	22	21	20	18
Ge	3	7	4	5	5	4	5	5	5	6	6	6
As	<5	33	<5	6	11	13	16	13	7	8	9	11
Sr	395	186	454	117	205	298	184	252	221	303	351	270
Y	23.2	43.2	31.5	55.3	23.9	18.7	21.9	20.9	30.7	25.7	21.2	19.4
Nb	5.3	10.1	7.3	11.2	39.9	35.5	42.0	41.7	51.6	53.2	43.2	45.5
Mo	1.7	1.6	<2	2.2	<1	<1	<1	<1	1.2	<2	172.7	172.2
Cd	<0.2	0.2	<0.2	0.3	0.3	<0.1	<0.1	0.5	0.3	<0.2	<0.1	0.3
Li	N/A	N/A	N/A	N/A	N/A	N/A	N/A	N/A	N/A	N/A	57.5	49.8
In	<0.2	<0.2	<0.2	<0.2	N/A	N/A	N/A	N/A	N/A	0.8	N/A	N/A
Sn	0.9	2.4	1.1	3.6	1.2	0.9	0.5	<1	1.9	1.3	1.7	1.6
Cs	<0.5	<0.5	<0.5	<0.5	0.9	0.8	1.1	0.7	0.5	<0.5	1.0	0.8
Be	1.0	1.8	0.7	1.7	2.0	1.2	1.4	1.0	1.4	1.7	0.8	0.2
Cu	18	40	28	<1	30	29	27	34	2	39	51	61
Li	67	78	43	29	52	31	60	55	49	46	<1	<1
Mn	2007	2448	1470	1887	2900	1371	2400	2141	1884	1596	1721	1935
Ni	65	53	83	15	71	50	62	67	25	69	63	73
Pb	<1	<1	<1	<1	<1	<1	<1	<1	<1	<1	<1	<1
Rb	31	10	10	18	38	74	79	24	21	14	40	20
Sc	33	50	26	35	26	24	27	27	17	23	28	29
Ti	9305	16486	12034	15805	9736	9992	11026	11070	11032	10138	11155	11428
Zn	97	131	107	117	143	72	92	94	123	96	87	93
La	16.21	19.55	15.24	28.89	38.53	37.25	41.55	40.37	46.23	55.12	46.33	41.22
Ce	33.67	42.98	34.49	68.80	82.15	77.96	87.78	84.76	89.94	108.40	92.68	94.03
Pr	4.62	5.99	4.87	9.74	9.74	9.02	9.65	10.25	11.00	12.13	10.58	9.81
Nd	21.58	29.32	22.88	46.64	38.14	35.26	37.76	39.82	40.98	45.77	41.23	37.31
Sm	4.91	8.10	6.17	11.60	6.91	6.13	6.56	7.20	7.39	8.24	6.62	6.73
Eu	1.40	2.36	1.89	4.13	1.72	1.48	2.03	1.77	2.18	1.89	2.09	1.33
Tb	0.73	1.42	0.97	1.83	0.92	0.75	0.80	0.79	1.02	0.92	0.84	0.78
Gd	5.23	8.77	6.59	12.00	6.04	5.30	5.53	5.73	6.83	6.38	5.98	5.33
Dy	4.77	8.94	6.02	10.76	5.28	3.38	4.63	4.44	5.73	4.95	3.94	4.15
Ho	0.83	1.66	1.22	2.16	0.99	0.77	0.86	0.83	1.18	0.92	0.89	0.80
Er	2.64	5.04	3.44	6.54	2.81	2.26	2.43	2.26	3.23	2.63	2.53	2.22
Tm	0.36	0.70	0.50	0.77	0.37	0.30	0.32	0.32	0.47	0.32	0.31	0.31
Yb	2.45	4.49	3.25	5.17	2.36	1.98	2.22	2.15	3.18	2.34	2.15	2.10
Lu	0.36	0.64	0.47	0.75	0.33	0.28	0.34	0.33	0.42	0.34	0.31	0.35
Hf	2.72	5.15	3.66	6.65	4.88	4.06	4.14	4.23	4.88	4.56	4.31	4.38
Ta	<0.5	0.69	<0.5	0.96	3.16	3.28	1.73	1.91	3.67	3.28	2.84	3.19
W	1.91	1.46	<1	1.71	2.17	1.23	1.58	1.05	1.94	<1	1.48	2.02
Tl	<0.1	<0.1	<0.1	<0.1	0.14	0.28	0.28	<0.1	<0.1	<0.1	0.14	<0.1
Bi	<0.4	0.61	<0.4	0.95	N/A	N/A	N/A	N/A	N/A	<0.4	N/A	N/A
Th	0.69	1.41	1.46	2.48	6.06	4.62	5.42	5.18	8.58	6.06	5.74	6.05
U	0.23	0.70	0.52	0.56	1.38	1.31	1.10	0.97	2.21	2.12	1.44	1.10

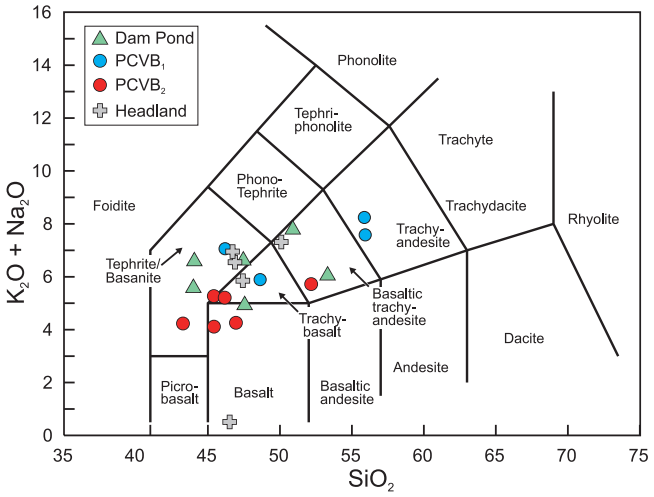

Figure 3. *Total alkalis* vs *silica diagram of Le Bas* et al. *(1986) showing the compositions of the three groups of basaltic rocks from the Bonavista Peninsula.*

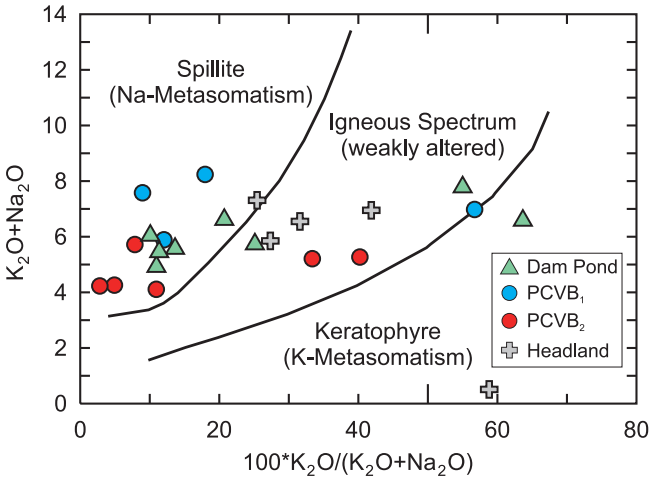

Figure 4. *Igneous spectrum plot of Hughes (1973). Samples to the left and right of the 'igneous spectrum' are likely compositionally altered.*

RARE-EARTH ELEMENT (REE) GEOCHEMISTRY

Variations in the basalt chemistry are plotted on REE and multi-element plots, normalized to chondrite (CN) and primitive mantle (PM), respectively (Figure 9) (normalizing values from Sun and McDonough, 1989). Samples of the Dam Pond basalt are more strongly fractionated than the Headland basalt and rocks from the PCVB, with $(La/Yb)_{CN}$ ratios ranging from 10.43 to 16.90 (Figure 9A) and $(Gd/Yb)_{CN}$ ratios ranging from 1.78 to 2.31. The Dam Pond samples have slight negative Eu anomalies (Eu/Eu* = 0.68-1.03; mean = 0.86), and minor Nb, Zr, and Hf troughs (Figure 9B).

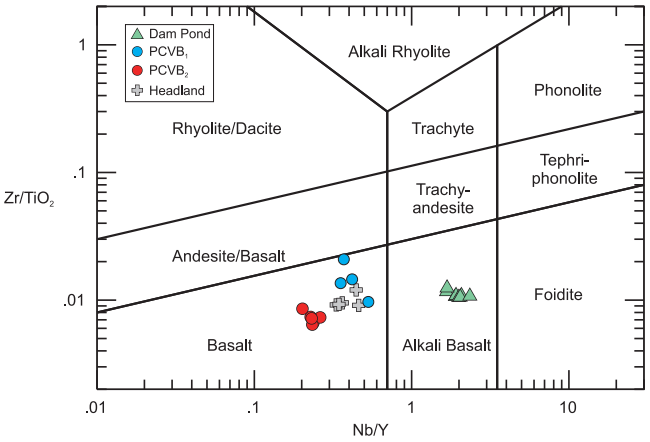

Figure 5. *Zr/TiO_2* vs *Nb/Y discrimination diagram after Pearce (1996; modified from Winchester and Floyd, 1977) showing the compositions of basaltic rocks from the Bonavista Peninsula.*

The Headland basalt samples have moderately fractionated REE patterns where $(La/Yb)_{CN}$ ranges from 10.91 to 14.94, $(Gd/Yb)_{CN}$ ranges from 2.43 to 2.93, and they have pronounced negative Nb anomalies (Figure 9D). The Headland samples have slight Eu troughs (Eu/Eu* = 0.84-0.98) and exhibit negative Zr–Hf and Ti anomalies.

The Plate Cove basalt samples have the flattest REE patterns of the three basalt units, where $(La/Yb)_{CN}$ ranges from 3.10 to 4.76. Most have slight negative Nb and Ti anomalies, with $PCVB_1$ rocks having higher Nb concentrations than $PCVB_2$ rocks (Figure 9F). Most PCVB samples have a weak negative Eu anomaly with Eu/Eu* values ranging from 0.78 to 1.22 for $PCVB_1$ and 0.83 to 1.07 for $PCVB_2$ (Figure 9E). Rocks of $PCVB_1$ differ from those of $PCVB_2$ in that the latter have slight depletions in Zr and Hf and the former have slightly higher Th and Nb abundances than the latter (Figure 9F).

VOLCANIC SUITE DIFFERENCES AND PRELIMINARY PETROGENETIC CONSTRAINTS

All of the analyzed basaltic rocks of the Bonavista Peninsula have moderate to low Mg#'s, Cr and Ni contents (Figure 7), and are, therefore, not primary melts of a depleted asthenospheric mantle (*e.g.,* Roeder and Emslie, 1970; Ringwood, 1975), but have likely undergone substantial fractionation in the crust. Field and preliminary petrographic and geochemical evaluation of the mafic volcanic rocks of the Bonavista Peninsula reveals that the three units (PCVB, HB and DP) are geochemically distinct (Figure 10A, B). The DP basalt samples are the most fractionated, are alkalic

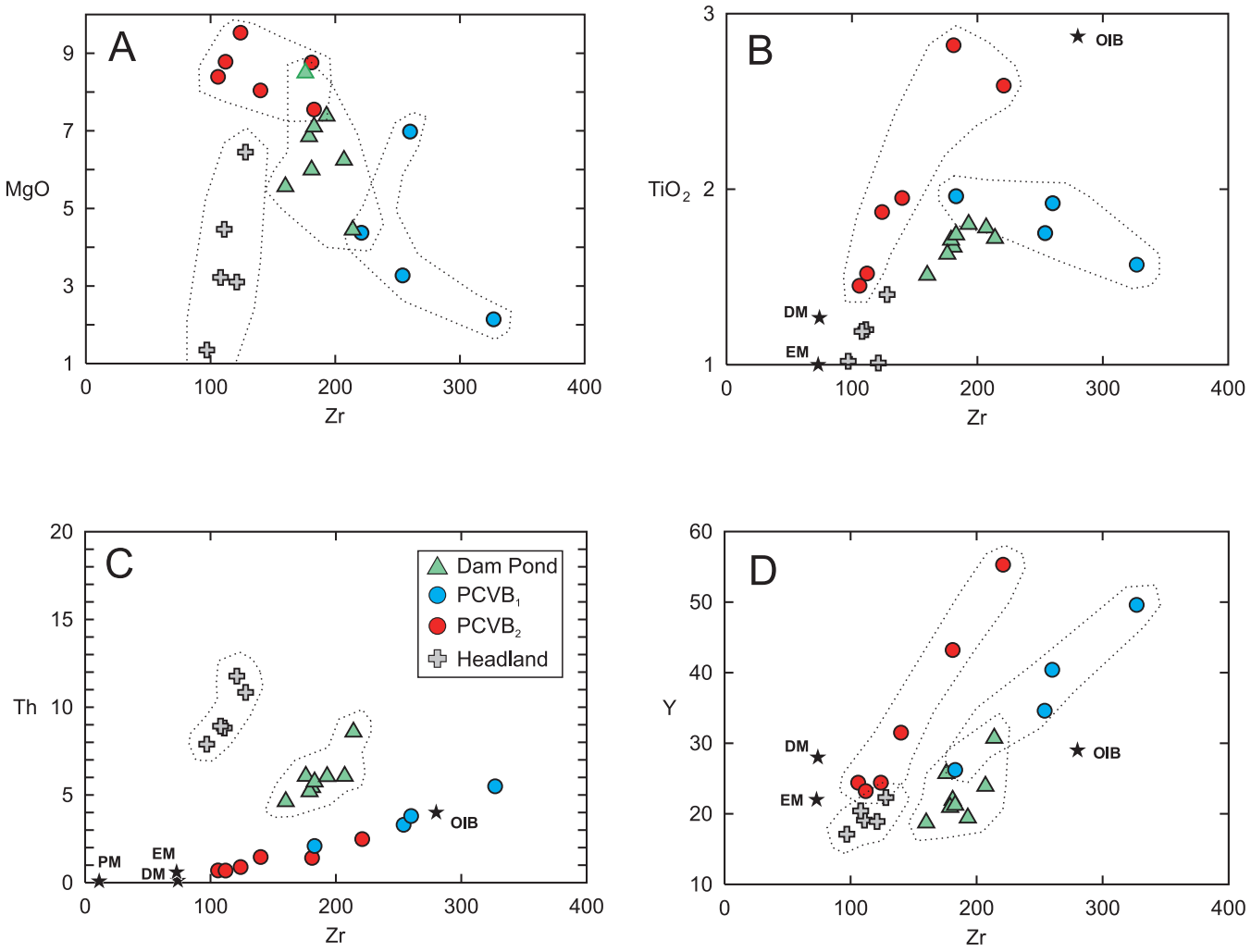

Figure 6. *Selected element-element diagrams: major oxides (in weight %) and trace elements (in ppm) plotted against Zr to show compositional variations.* See *text for details. DM = depleted mantle; EM = enriched mantle; PM = primitive mantle; OIB = ocean island basalt; from Sun and McDonough (1989).*

and plot well into the enriched side of the MORB array (Figure 10A), owing to their high Nb/Yb. Their position well to the right of the diagram (Figure 10A) and just above the MORB array shows that, relative to the two other units, the alkaline, OIB-like DP basalt has elevated Nb/Yb and moderate TiO_2/Yb, and likely originated from a lower degree of melting at greater depth, likely with minor residual garnet (Figure 10A; Pearce, 2008). Although the DP samples plot proximal to the MORB–OIB array, minor lithospheric contamination is inferred from their displacement above the MORB–OIB array and their high Th contents (Figure 10B).

Both the PCVB and HB plot within the enriched MORB array, albeit at lower Nb/Yb and significantly closer to N-MORB than the DP basalts (Figure 10A). $PCVB_1$ and $PCVB_2$ define two parallel arrays (Figure 10A, B). These two arrays support the existence of two distinct series of chemically similar basaltic rocks, each derived from slightly different, variably enriched, shallow asthenospheric sources. The two PCVB subunits appear to have formed from polybaric fractional crystallization of clinopyroxene and plagioclase (Pearce, 2008). Both PCVB subunits also show similar amounts of crustal contamination in terms of their variable but elevated Th/Yb, yet each subunit has a distinct mantle source, as shown by their differing Nb/Yb (Figure 10A and B). In contrast, the HB have the highest Th/Yb ratio and show the greatest amount of lithospheric recycling (Figure 10B). These incompatible element relationships indicate that the HB are large-ion lithophile element (LILE)-enriched and were erupted in a mature, continental subduction setting (Pearce, 1982, 2008).

CONCLUSIONS

Field, petrographic and lithogeochemical observations provide new data on the nature and setting of the three mafic

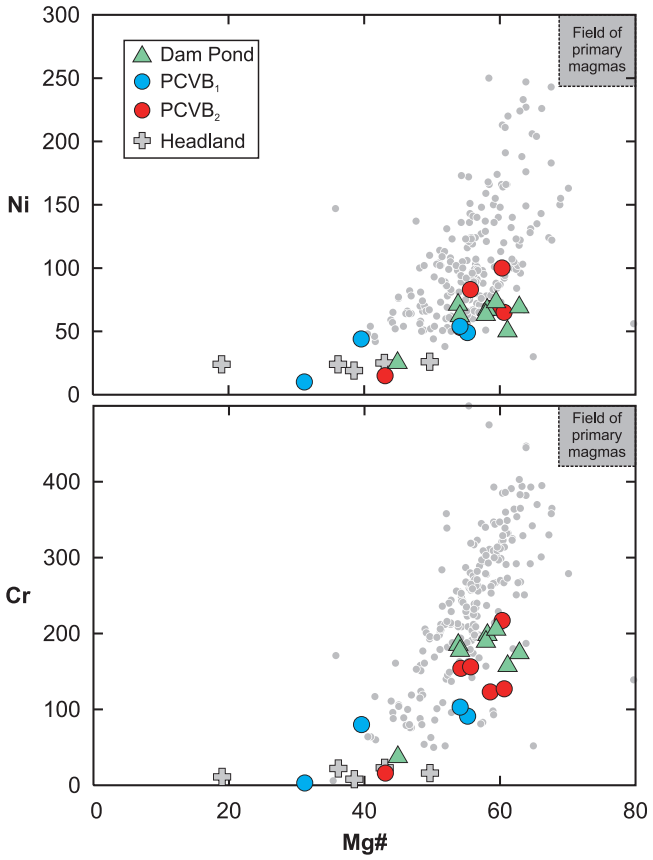

Figure 7. *Cr (ppm) and Ni (ppm)* vs *Mg# for basaltic rocks of the Bonavista Peninsula. Shown for comparison are data for global, normal mid-ocean ridge basalts (grey dots: Lenhert* et al.*, 2000) and for approximate fields of primary mantle-derived melts (*e.g.*, Roeder and Emslie, 1970; Ringwood, 1975).*

volcanic units from the Bonavista Peninsula. The Dam Pond basalt samples show no significant depletion in HFSE (Figure 9B), but are LREE- and LILE-enriched, have a within plate signature (Figure 8A, B) and are chemically similar to alkali OIB, albeit with slightly elevated Th. They likely formed as low degree partial melts of enriched mantle at depths greater than 60 km (Pearce, 2008).

The HB are LILE- and LREE-enriched basalts with deep HFSE troughs (Figure 9D) and are volcanic arc basalts (Figure 8A, B) that erupted in a mature continental subduction setting. The evolution of the PCVB is more complex. At least two distinct magmatic series are evident, both derived from an enriched MORB source. Both PCVB subunits are interpreted to represent transitional, arc-like to E-MORB-like basalts that most commonly form in marginal basins (Pearce, 1996).

Given the clear geochemical differences, a proposed correlation of the DP unit with the PCVB suggested by Normore (2010) is unlikely. Although their exposure is limited, a magnetic high running north-northeast along the eastern Bonavista Peninsula, west of the SC–EH fault, suggests that the volcanic rocks at Dam Pond may be more extensive in the subsurface (Figure 4, Normore, 2010) but their stratigraphic position remains poorly constrained.

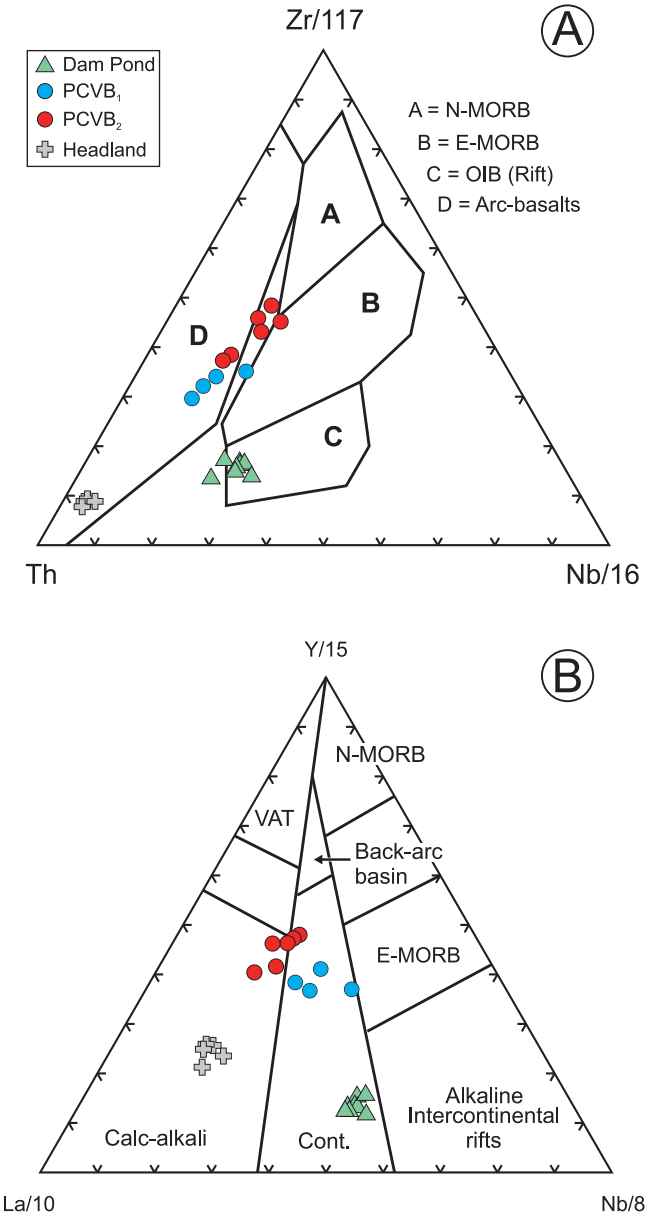

Figure 8. *A) Ternary plot of Th-Nb/16-Zr/117, as tectonic discrimination diagram (Wood, 1980); and B) tectonic discrimination diagram of Cabanis and Lecolle (1989).*

The results of this investigation highlight the need for modern trace-element data to aid in the correlation of volcanic suites of the Avalon Zone, particularly those currently mapped as Bull Arm Formation. Existing geochemical data from the type area of the BAF (Isthmus of Avalon; Figure 1)

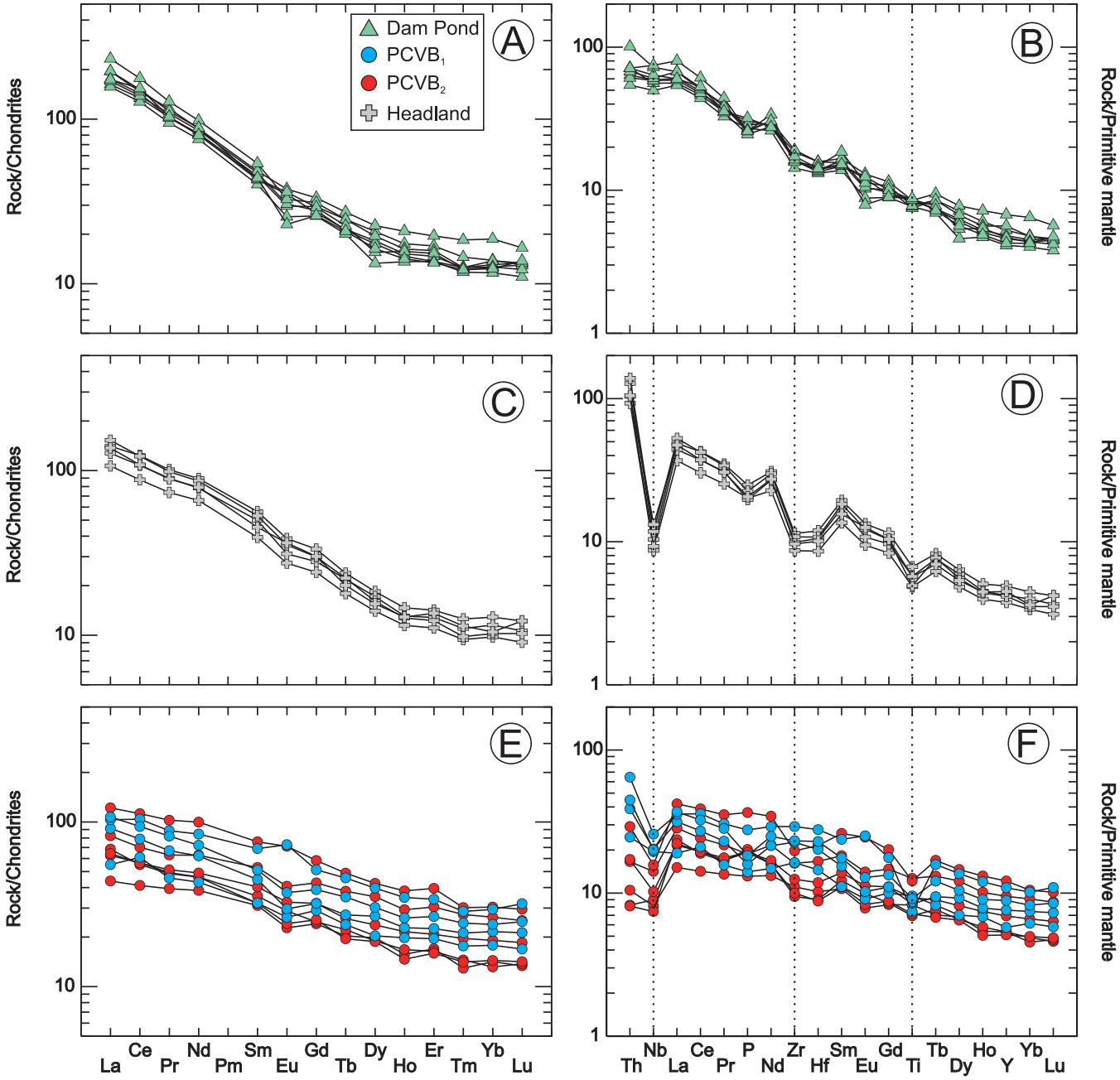

Figure 9. *Chondrite-normalized (as per Sun and McDonough, 1989) REE and primitive-mantle-normalized extended-REE patterns for basaltic rocks of the Bonavista Peninsula.*

include only four trace elements, most of which are now known to be mobile (*e.g.*, Rb, Sr, Ba (mobile), and Zr (immobile); (Malpas, 1972)). To fully evaluate the correlation of mafic volcanic rocks in the Bonavista region to those of the BAF, a comprehensive lithogeochemical program will need to be developed and implemented. It is clear from the above data that the origin of the mafic volcanic rocks in the region is far more complicated than previously recognized.

ACKNOWLEDGMENTS

Chris Finch is thanked for timely delivery of the lithogeochemical results from archived samples. Kim Morgan is thanked for drafting the map figures. Thoughtful reviews by Alana Hinchey and Tim van Nostrand helped to improve the manuscript.

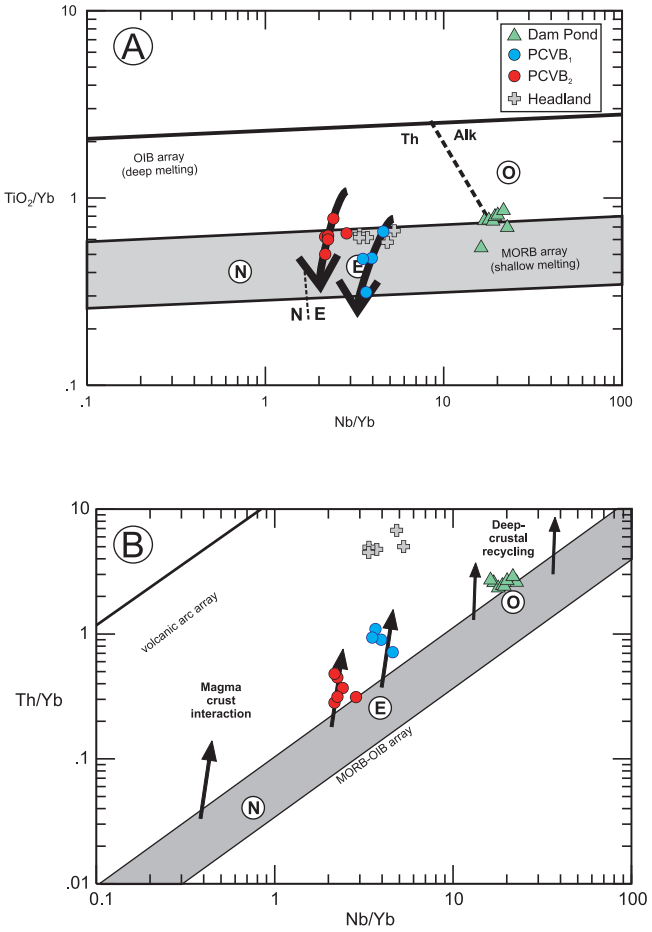

Figure 10. *A) TiO_2/Yb* vs *Nb/Yb; and B) Nb/Yb* vs *Th/Yb (after Pearce, 2008) for basaltic rocks of the Bonavista Peninsula. Key: N = N-MORB; E = E-MORB; O = ocean island basalt (Sun and McDonough, 1989).*

REFERENCES

Cabanis, B. and Lecolle, M.
1989: Le diagramme La/10-Y/15-Nb/8: un outil pour la discrimination des series volcaniques et la mise en evidence des processus de mélange et/ou de contamination crustale. Comptes Rendus de l'Acadamie des Sciences, Series II, Volume 309, pages 2023-2029.

Christie, A.M.
1950: Geology of Bonavista map-area, Newfoundland (summary account). Department of Mines and Technical Surveys. Geological Survey of Canada. Paper 50-7, 40 pages [002C/0007].

Finch, C.J.
1998: Inductively coupled plasma-emission spectrometry (ICP-ES) at the Geochemical Laboratory. *In* Current Research. Newfoundland Department of Mines and Energy, Geological Survey, Report 98-1, pages 179-193.

Fletcher, T.P.
2006: Bedrock geology of the Cape St. Mary's peninsula, southwest Avalon Peninsula, Newfoundland. Department of Natural Resources, Geological Survey, Report 06-02, pages 1-115.

Hayes, A.O.
1948: Geology of the area between Bonavista and Trinity bays, eastern Newfoundland. Geological Survey of Newfoundland, Bulletin 32 (Part 1), pages 1-37.

Hofmann, H.J., O'Brien, S.J. and King, A.F.
2008: Ediacaran biota on Bonavista Peninsula, Newfoundland, Canada. Journal of Paleontology, Volume 82, Number 1, pages 1-36.

Hughes, C.J.
1973: Spilites, keratophyres, and the igneous spectrum. Geological Magazine, Volume 109, pages 513-527.

Jenness, S.E
1963: Terra Nova and Bonavista map-areas, Newfoundland (2D E ½ and 2C). Geological Survey of Canada, Memoir 327, 184 pages.

King, A.F., Anderson, M.M. and Benus, A.P.
1988: Late Precambrian sedimentation and related orogenesis of the Avalon Peninsula, eastern Avalon Zone. Geological Association of Canada, St. John's 1988 Field Trip Guidebook, A4, pages 1-84.

Le Bas, M.J., Le Maitre, R.W., Streckeisen, A. and Zanettin, B.
1986: A chemical classification of volcanic rocks based on the total alkali silica diagram. Journal of Petrology, Volume 27, Number 3, pages 745-750.

Lehnert, K., Su, Y., Langmuir, C., Sarbas, B. and Nohl, U.
2000: A global geochemical database structure for rocks. Geochemistry Geophysics Geosystems 1, Paper number 1999GC000026.

Malpas, J.G.
1972: The petrochemistry of the Bull Arm Formation near Rantem Station, Southeast Newfoundland. Unpublished M.Sc. thesis, Memorial University of Newfoundland, 126 pages.

McCartney, W.D.
1967: Whitbourne map area, Newfoundland, Geological Survey of Canada, Memoir 341, 135 pages.

Middelburg, J.J., Van der Weijden, C.H. and Woittiez, J.R.W.
1988: Chemical processes affecting the mobility of major, minor and trace elements during weathering of granitic rocks. Chemical Geology Volume 68, pages 253-273.

Mills, A.J.
2014: Preliminary results from bedrock mapping in the Sweet Bay area (parts of NTS map areas 2C/5 and 2C/12), western Bonavista Peninsula, Newfoundland. *In* Current Research. Newfoundland and Labrador Department of Natural Resources, Geological Survey, Report 14-1, pages 135-154.

Nesbitt, H.W. and Young, G.M.
1982: Early Proterozoic climates and plate motions inferred from major element chemistry of lutites. Nature, Volume 299, pages 715-717.

Normore, L.S.
2010: Geology of the Bonavista map area (NTS 2C/11), Newfoundland. *In* Current Research. Newfoundland and Labrador Department of Natural Resources, Geological Survey, Report 10-1, pages 281-301.

2011: Preliminary findings on the geology of the Trinity map area (NTS 2C/06), Newfoundland. *In* Current Research. Newfoundland and Labrador Department of Natural Resources, Geological Survey, Report 11-1, pages 273-293.

O'Brien, S.J.
1994: On the geological development of the Avalon Zone in the area between Ocean Pond and Long Islands, Bonavista Bay (parts of NTS 2C/5 and NTS 2C/12). *In* Current Research. Newfoundland Department of Mines and Energy, Geological Survey, Report 94-1, pages 187-199.

O'Brien, S.J., Dunning, G.R., Knight, I. and Dec, T.
1989: Late Precambrian geology of the north shore of Bonavista Bay (Clode Sound to Lockers Bay). *In* Report of Activities. Geological Survey Branch, Department of Mines and Energy, pages 49-50.

O'Brien, S.J. and King, A.F.
2002: Neoproterozoic stratigraphy of the Bonavista Peninsula: preliminary results, regional correlations and implications for sediment-hosted stratiform copper exploration in the Newfoundland Avalon Zone. *In* Current Research. Newfoundland Department of Mines and Energy, Geological Survey, Report 02-1, pages 229-244.

2004a: Ediacaran fossils from the Bonavista Peninsula, Newfoundland: preliminary descriptions and implications for correlations. *In* Current Research. Newfoundland Department of Mines and Energy, Geological Survey, Report 04-1, pages 203-212.

2004b: Late Neoproterozoic to earliest Paleozoic stratigraphy of the Avalon Zone in the Bonavista Peninsula, Newfoundland: an update. *In* Current Research. Newfoundland Department of Mines and Energy, Geological Survey, Report 04-1, pages 213-224.

2005: Late Neoproterozoic (Ediacaran) stratigraphy of the Avalon Zone sedimentary rocks, Bonavista Peninsula, Newfoundland. *In* Current Research. Newfoundland and Labrador Department of Natural Resources, Geological Survey, Report 05-1, pages 101-114 [NFLD/2903].

O'Brien, S.J., King, A.F. and Hofmann, H.J.
2006: Lithostratigraphic and biostratigraphic studies on the eastern Bonavista Peninsula: an update. *In* Current Research. Newfoundland and Labrador Department of Natural Resources, Geological Survey, Report 06-1, pages 257-263.

Pearce, J.A.
1982: Trace element characteristics of lavas from destructive plate boundaries. *In* Andesites. *Edited by* R.S. Thorpe. John Wiley and Sons, New York, 724 pages.

1996: A user's guide to basalt discrimination diagrams. *In* Trace Element Geochemistry of Volcanic Rocks; Applications for Massive Sulphide Exploration. Short Course Notes, Geological Association of Canada, Volume 12, pages 79-113.

2008: Geochemical fingerprinting of oceanic basalts with applications to ophiolite classification and the search for Archean oceanic crust. Lithos, Volume 100, pages 14-48.

Pearce, J.A. and Cann, J.R.
1973: Tectonic setting of basic volcanic rocks determined using trace element analyses. Earth and Planetary Science Letters, Volume 19, pages 290-300.

Ringwood, A.E.
1975: Composition and petrology of the Earth's mantle. McGraw-Hill Book Co., New York, N.Y., USA, 618 pages.

Roeder, P.L. and Emslie, R.F.
1970: Olivine-liquid equilibrium. Contributions to Mineralogy and Petrology, Volume 29, pages 275-289.

Rose, E.R.
1948: Geology of the area between Bonavista, Trinity, and Placentia bays, eastern Newfoundland. Geological Survey of Newfoundland, Bulletin 32 (Part 2), pages 41-48.

Spitz, G. and Darling, R.
1978: Major and minor element lithogeochemical anomalies surrounding the Louvem copper deposit, Val d'Or, Quebec. Canadian Journal of Earth Sciences, Volume 15, Number 7, pages 1161-1169.

Sun, S.S. and McDonough, W.F.
1989: Chemical and isotopic systematics of oceanic basalts: implications for mantle composition and processes. *In* Magmatism in the Ocean Basin. *Edited by* A.D. Saunders and M.J. Norry. Geological Society of London, Special Publication 42, pages 313-345.

Winchester, J.A. and Floyd, P.A.
1977: Geochemical discrimination of different magma series and their differentiation products using immobile elements. Chemical Geology, Volume 20, pages 325-343.

Wood, D.A.
1980: The application of a Th-Hf-Ta diagram to problems of tectomagmatic classification and to establishing the nature of crustal contamination of basaltic lavas of the British Tertiary Volcanic Province. Earth and Planetary Science Letters, Volume 50, pages 11-30.